

Application of Fluid-Mechanical Interaction in Stability Analysis of Underground Connection Way Excavation

Jin-Yueih Bair

Rouh Yur Office of Engineering Technology Affairs

jybair88@gmail.com

ABSTRACT

The interaction between fluid and solid is generally called fluid-solid coupling, and geotechnical problems often involve groundwater, seepage or excess pore water pressure. The change of pore water pressure leads to the change of effective stress, which affects the mechanical properties of the soil. The reduction of effective stress may make the soil achieve plastic yield; and the fluid in the soil will react to the change of soil volume, which is expressed as In this study, FLAC3D was used to conduct uncoupled and coupled calculations for the excavation of a connection way in Taiwan, in order to understand the influence of fluid-solid interaction on the excavation stability of the connection way.

KEYWORDS: fluid-mechanical coupling, seepage

1. Introduction

Interaction between fluid and solid generally is called fluid-mechanical coupling. Geotechnical issues often involve flow of fluid and seepage or excess pore pressure in soil. First, changes of pore water pressure leads to changes in effective stresses, which affect the response of the solid (for example, a reduction in effective stress may induce plastic yield). Second, the fluid in a zone reacts to mechanical volume changes by a change in pore pressure.

The connection way goes through the sandy silt (ML). The soil consists of inorganic silts and very fine sands. The groundwater level is 1.2 m below the pavement surface. For the connection way, the neglect of vertical stress increase with depth due to gravity is not justified. Thus, the in-situ stress based on hydrostatic primary stress are not applicable. In the shallow tunnels, the soil is not cohesive material and the daylight collapse may occur during the tunnelling. For the safety, the assessment of the variation of pore pressure around the connection way during the tunnelling is necessary.

In addition, fine particles in the soil may be taken away by the seepage and causes the collapse at the face. The assessment of the grouting along the connecting way is also necessary. There are two cases of numerical analysis done. One is without the grouting along the connection way in numerical analysis. The other is with along the connection way in numerical analysis. The flow modelling in FLAC^{3D} is used to capture the effects of fluid/solid interaction. Fig.1 is the layout of the connection way.

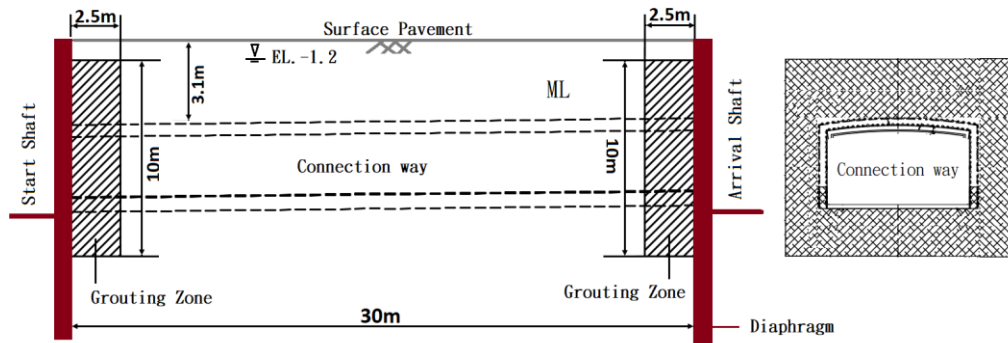


Fig. 1. Underground connection way configuration

2. Geology

The research base is located at the foot of the west side of the Baguashan platform, as shown in Fig. 2. According to the drilling report, from the surface to 34 meters below the surface is silty clay. Below the silty clay is the layer of pebbles. The average N value from the surface to 15 meters below the surface is 6. The average N value from 15 meters to 34 meters below the surface is 18. Groundwater is located 1 meter above the surface.

The alluvial deposits in the Changhua Plain mainly come from the Zhuoshui River at the southern end, and the amount of sand transported by the Zhuoshui River far exceeds that of other rivers on Taiwan's main island (Encyclopedia of Taiwan, Ministry of Culture). The base is located in the uplifted coastal plain of Changhua. The Zhuoshuixi alluvial plain covers the Changhua uplift coastal plain, formed by modern alluvium hundreds of meters thick. Alluvium consists of gravel, sand, silt and clay. The alluvium is Holocene non-marine alluvium. According to the geological drilling report, from the surface to 34 meters below the surface is silty clay, below which is a pebble layer. Since the thick clay layer is formed by marine or abyssal sedimentary environment, the silty clay soil from the surface to 34 meters below the surface should be sandy silt (ML).



Figure 2. Geological map of the base area

3. Soil geotechnical parameters

The geotechnical parameters of unimproved soil layer are shown in Table 1. Seepage analysis parameters of unimproved soil layer are shown in Table 2. Soil particles are assumed to be incompressible. The soil permeability coefficient before improvement is $k=1 \times 10^{-4}$ cm/sec. The soil permeability coefficient after improvement is $k=1 \times 10^{-5}$ cm/sec. After improvement, the cohesion of the soil layer is 2 kgf/cm^2 and the friction angle is 14° . The elastic modulus and bulk modulus of the improved soil layer remain unchanged.

According to the analysis of soil particle size, the uniformity coefficient and curvature coefficient of the soil particle size distribution from the surface to 20 meters below the surface are shown in Table 3. Underground seepage may cause seepage deformation to the soil, such as soil flow or piping (Wan Lianju et al. 2001). The soil porosity $n=0.367$, fine particle volume is equal to skeleton pore volume $P_z=0.95 \frac{\sqrt{n}}{1+\sqrt{n}} = 0.36$. The soil of this base is sandy silt, and seepage and deformation of the soil caused by groundwater seepage may become soil flow (Figure 3).

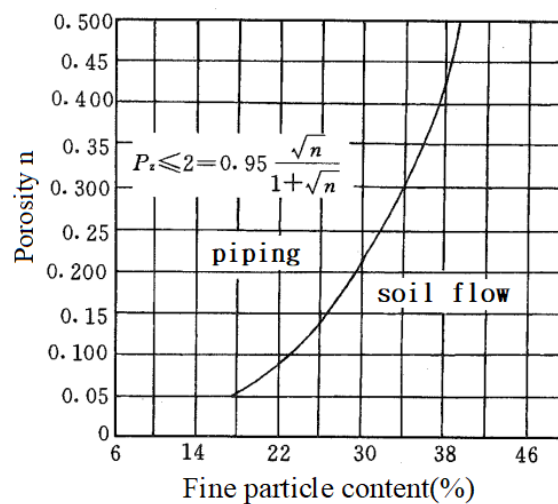


Figure 3. Discriminant soil flow and piping diagram

Table 1. Geotechnical parameters

Depth(m)	Soil layer	N	ρ_t (t/m ³)	W _n (%)	n	c' (tf/m ²)	ϕ '(°)	Elastic modulus (tf/m ²)	Poisson's ratio
0~34	sandy silt	9	1.95	18.4	0.367	0	28	675	0.35
below 34	gravel	50	2.1	-	-	0	38	-	-

Table 2. Seepage analysis parameters of unimproved soil layer

Depth (m)	Soil layer	Permeability coefficient (cm/s)	Dry density (t/m ³)	Biot coefficient α	Biot modulus M (tf/m ²)	Fluid modulus K _f (tf/m ²)	Soil modulus K (tf/m ²)	Undrained soil modulus K _u (tf/m ²)
0~34	sandy silt	1.0E-04	1.65	1	5.45E+08	2.00E+08	7.50E+06	5.52E+08

Table 3. Uniform coefficient and curvature coefficient of soil particle size distribution (mm)

d ₆₀	d ₃₀	d ₁₀	c _u	c _c	Deformation
0.140	0.070	0.0230	6.1	1.5	soil flow
0.078	0.030	0.0063	12.4	1.8	soil flow or piping
0.058	0.013	0.0063	9.2	0.5	soil flow
0.170	0.075	0.0400	4.3	0.8	soil flow
0.048	0.020	0.0040	12.0	2.1	soil flow or piping
0.052	0.023	0.0070	7.4	1.5	soil flow
0.028	0.010	0.0030	9.3	1.2	soil flow

4. Analysis model

The analysis model is shown in Figure 4. Uniaxial compressive strength of the diaphragm is 280kgf/cm². Its elastic modulus is 2.51×10⁵kgf/cm² and Poisson's ratio is 0.35. Uniaxial compressive strength of the shotcrete with a thickness of 35cm is 210kgf/cm². Its elastic modulus is 2.17×10⁵kgf/cm² and Poisson's ratio is 0.35. Elastic modulus of the steel supports 250×9×14 is 2040tf/cm² and its yield strength is 2.5tf/cm². Elastic modulus of the ϕ 114.3mm steel pipes is 2040tf/cm² and its yield strength is 2.5tf/cm². Tensile strength of the ϕ 114.3mm face pipes is 200kgf/cm². Mechanical properties of the horizontal face pipes and steel pipes used in the numerical analysis are shown in Table 4.

Each round of pure excavation time t_s is 4 hours. According to Table 1 and Table 2, the characteristic time t_c of the fluid diffusion process of the unimproved soil and the soil after geological improvement is calculated (Table 5 and Table 6). Since t_s is within the range of t_c , during the excavation process, the time required for groundwater seepage length L_c is approximately equal to the pure excavation time t_s of each round. Fluid-mechanical coupling analysis (CONFIG fluid, SET fluid on mech on) is used. The diaphragm is set as an impermeable material, and the sides and bottom of the model are set as fixed hydraulic pressure boundaries (permeable boundaries). The distribution of pore pressure before the excavation is shown in Figure 5.

Before the excavation of the connection passage, the grouting improvement is carried out at the start end and the arrival end. The scope of the grouting improvement is shown in Figure 1. Advance length of the underground connection way is 1 meter.

For every 6 meters of excavation of the connection way, 12 meters of steel pipes and face pipes are installed.

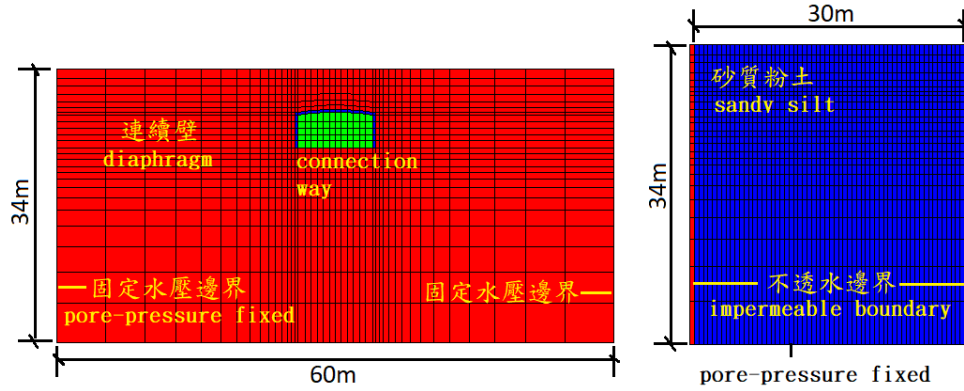


Figure 4. Analysis model

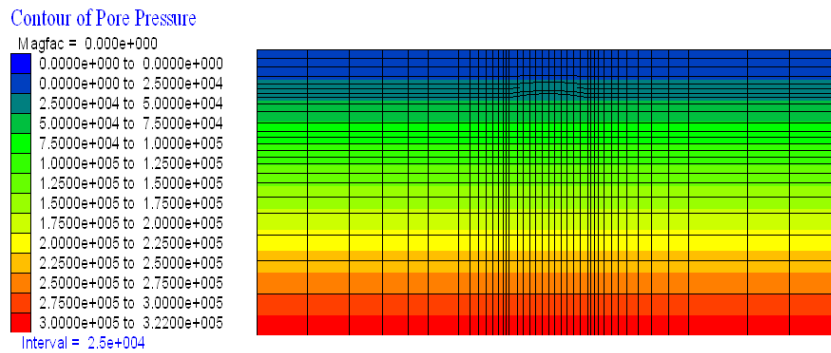


Figure 5. Distribution of pore pressure before the connection way excavation

Table 4. Mechanical properties of the face pipes and steel pipes(Bair 2020)

Property	Steel pipe	Face pipe
emod E (N/m ²)	2.1E+11	8.0E+8
nu μ	0.2	0.38
xcarea A (m ²)	0.00204	0.000717
perimeter p (m)	0.35908	0.11938
xciy I _x (m ⁴)	3.0E-06	9.6E-08
xciz I _y (m ⁴)	3.0E-06	9.6E-08
xcj J (m ⁴)	6.0E-06	1.92E-07
cs_scoh c _s (N/m)	9.3E+03	3.0E+04
cs_sfric ψ_s (°)	19.0	14.0
cs_sk E _s (N/m ²)	2.2E+11	8.0E+10
cs_ncoh c _n (N/m)	6.0E+05	8.4E+08
cs_nfric ψ_n (°)	34.0	34.0
cs_nk E _n (N/m ²)	3.5E+07	1.07E+07
Tfstrain ϵ_t	0.0004	0.0021
tyeild t _y (N)	8.57E+05	5E+04

Table 5. Seepage characteristics of unimproved soil

Item	Characteristic time $L_c(m)$	Cycle time $t_s(sec)$	Characteristic time of the diffusion process $t_c(sec)$	Storativity	Diffusivity $c(m^2/sec)$
Flow-only mode	2	1.44E+04	7.20E+03	1.84E-09	5.56E-04
Coupled flow-mechanical	2	1.44E+04	5.30E+05	1.35E-07	7.55E-06

Table 6. Seepage characteristics of improved soil

Item	Characteristic time $L_c(m)$	Cycle time $t_s(sec)$	Characteristic time of the diffusion process $t_c(sec)$	Storativity	Diffusivity $c(m^2/sec)$
Flow-only mode	2	1.44E+04	7.20E+04	1.84E-09	5.56E-05
Coupled flow-mechanical	2	1.44E+04	5.30E+05	1.35E-07	7.55E-07

5. Numerical analysis results

5.1 Flow-only and unimproved soil

Without considering the fluid-mechanical coupling, after the first round of excavation of the connection way, the excavation face collapsed, as shown in Figure 6.

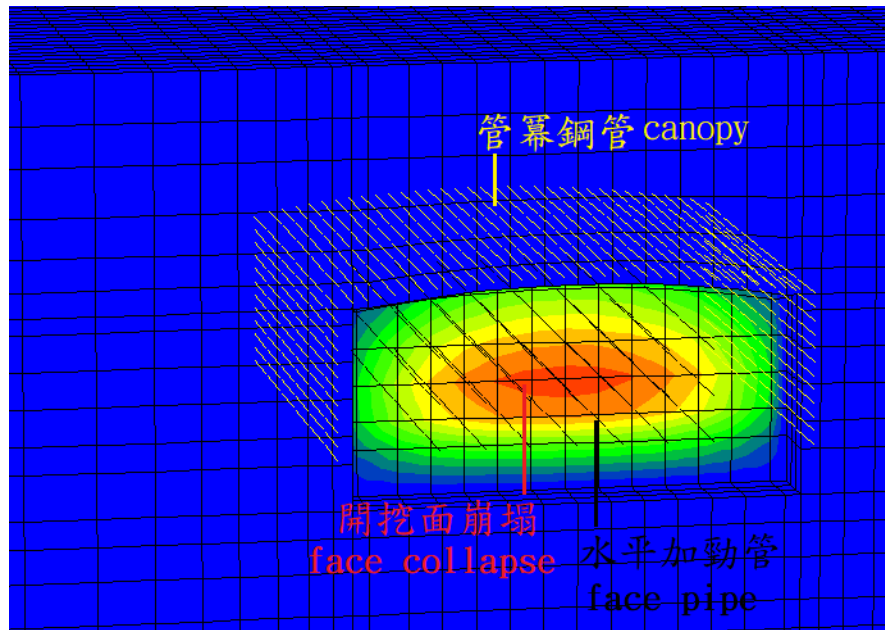


Figure 6. Face collapsed after the first round of excavation of the connection way

5.2 Coupled flow-mechanical mode

5.2.1 Grouting at start end and arrival end

After the third round of excavation, the face collapsed and had a subsidence of about 150 mm on the road pavement (see Figure 1). The distribution of pore pressure after the third round of excavation is shown in Figure 7. Due to the infiltration of groundwater into the excavation surface, the pore pressure around the roof of the connection way drops. The pore pressure about 13 meters away from the start end will not be affected by the excavation of the connection way. The seepage force is about $2.54 \times 10^3 \text{ N/m}^3$ and fine particles of the soil may be taken away by the seepage.

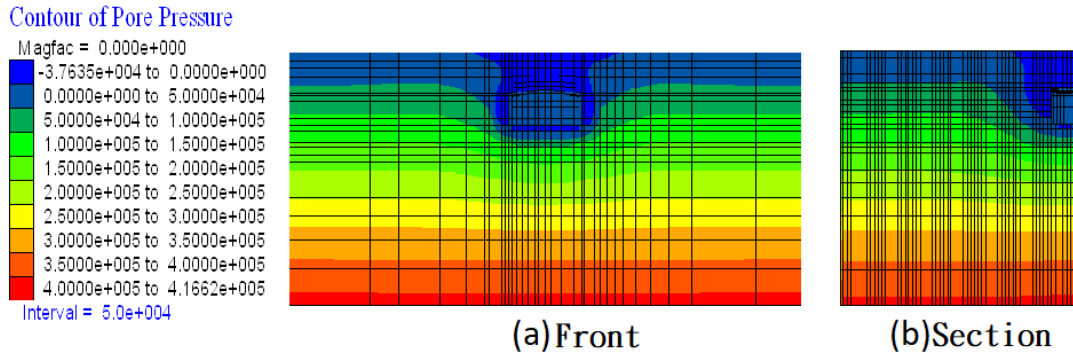


Figure 7. Distribution of groundwater pressure after the third round of excavation

5.2.2 Grouting around the entire connection way

For grouting around the entire connection way, the faces are stable and the maximum surface subsidence is about 15 mm. Figure 8 shows the variation of pore pressure behind the face. The pore pressure at 0.5 meters behind the face is zero, and the pore water pressure at 3.5 meters behind the face is $3.7 \times 10^3 \text{ N/m}^2$. The seepage force is about $1.06 \times 10^3 \text{ N/m}^3$. Since the sandy silt is cohesive after being improved by the grouting, it can prevent the fine particles from being taken away by the seepage force of groundwater.

Figure 9 shows the change of pore pressure at 3 meters above the roof during excavating the connection way. The pore pressure is negative after the completion of the excavation.

Figure 10 shows the change of pore pressure at a distance of 2.8 meters from the side wall during excavating the connection way. The pore pressure drops from $9.5 \times 10^4 \text{ N/m}^2$ to $2.7 \times 10^4 \text{ N/m}^2$, nearly 70% drop.

Figure 11 shows the change of pore pressure at 2.3 meters below the invert during excavating the connection way, nearly 66% drop.

Based on theory of poroelasticity (Arnold 2016, Andi 2002), we have $\frac{\partial p}{\partial t} = \frac{-\nabla \cdot \vec{q}}{S} - \frac{\alpha}{S} \frac{\partial \varepsilon}{\partial t}$. p is pore pressure. S is storativity. α is Biot coefficient. ε is volume strain. q is fluid flux. Farther away from the face, the soil is disturbed, causing the compression of the soil to be greater than the seepage of groundwater, thus causing the pore pressure above and on the side wall of the connection way to rise. The rise in pore pressure in Figure 9 (above the roof) is greater than the increase in pore water pressure in Figure 10 (side wall), which means that the soil above the roof is more disturbed than the soil near the side wall. This phenomenon can explain the possible failure mode of the connection way (Figure 12(b)). In Figure 12, h is the estimated possible collapse height, and Z_0 is the depth of the overburden.

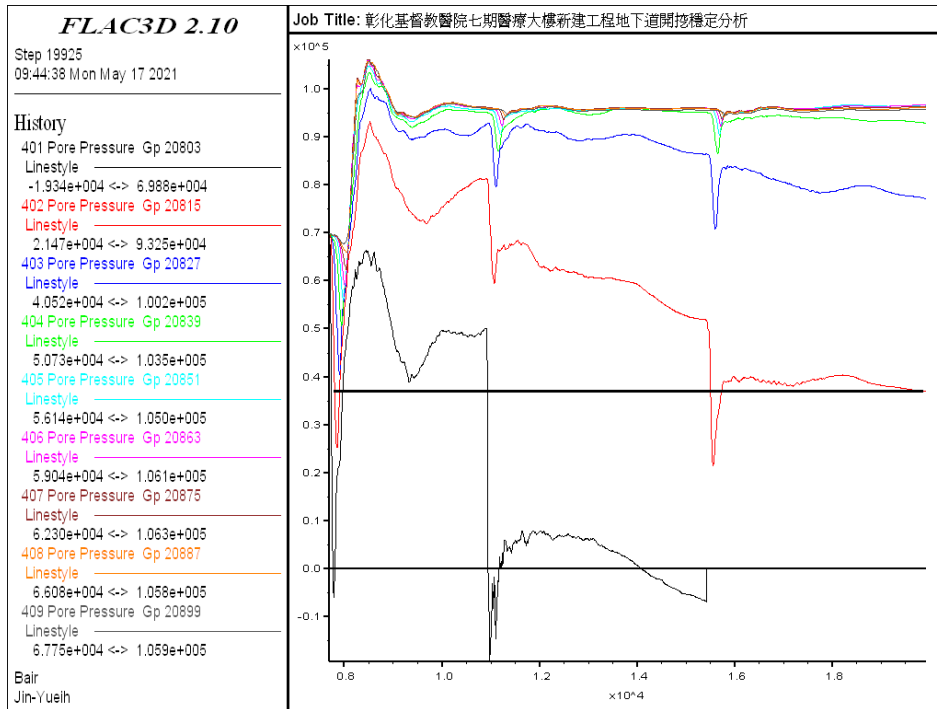


Figure 8. Variation of pore pressure behind the face in the third round

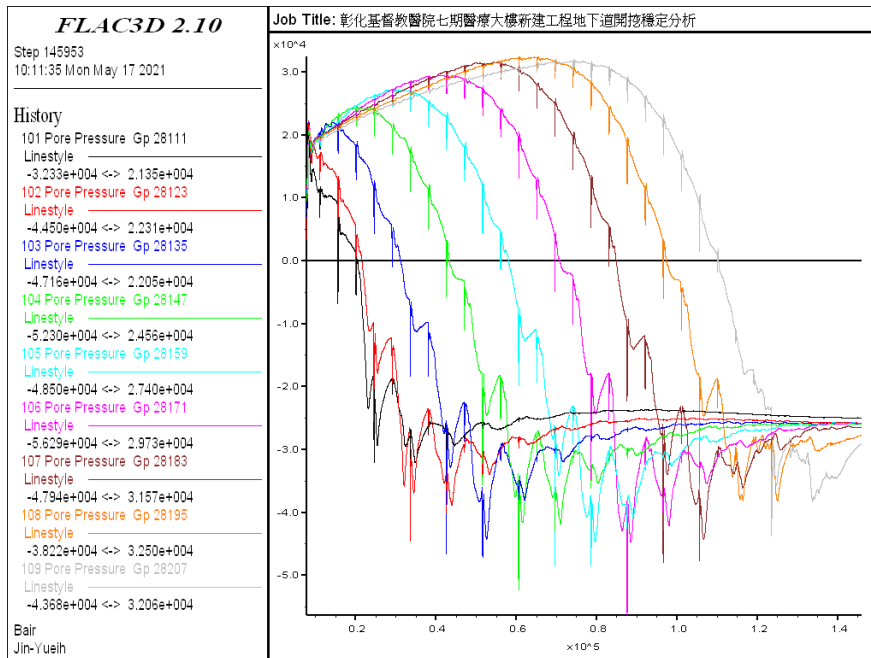


Figure 9. Variation of pore pressure at 3 meters above the roof of the connection way

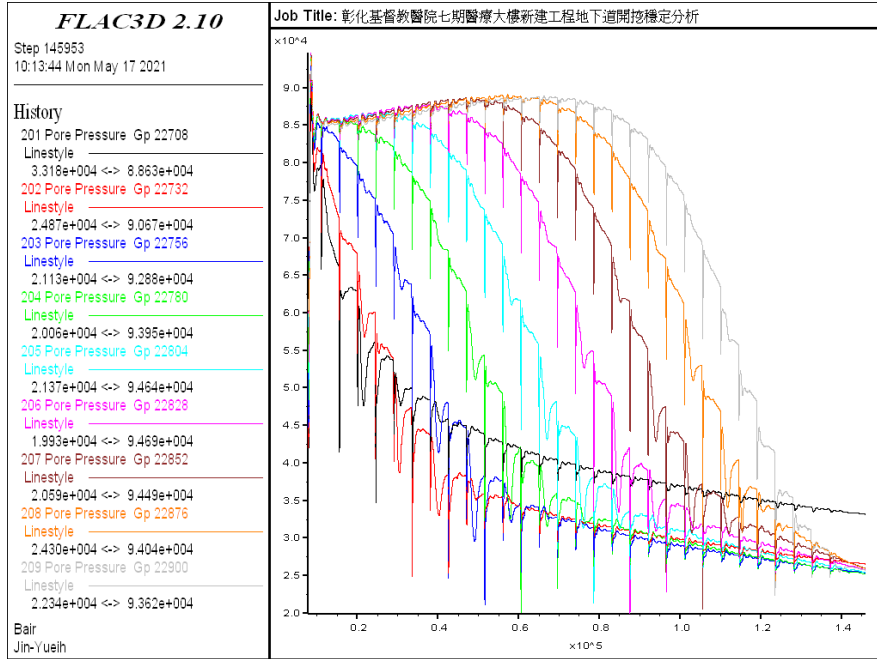


Figure 10. Variation of pore pressure at 2.8 meters on the side wall of the connection way

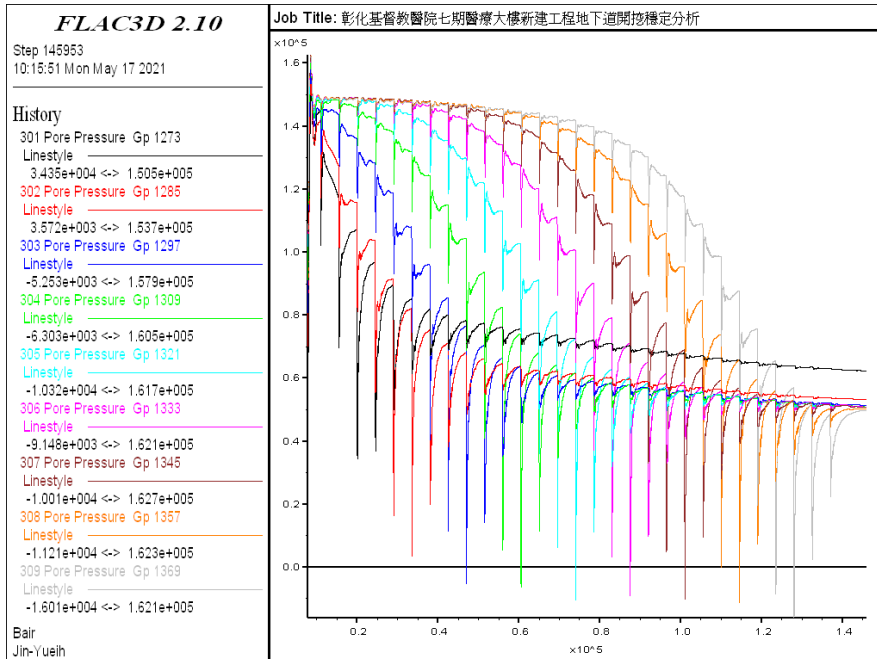


Figure 11. Variation of pore pressure at 2.3 meters below the invert of the connection way

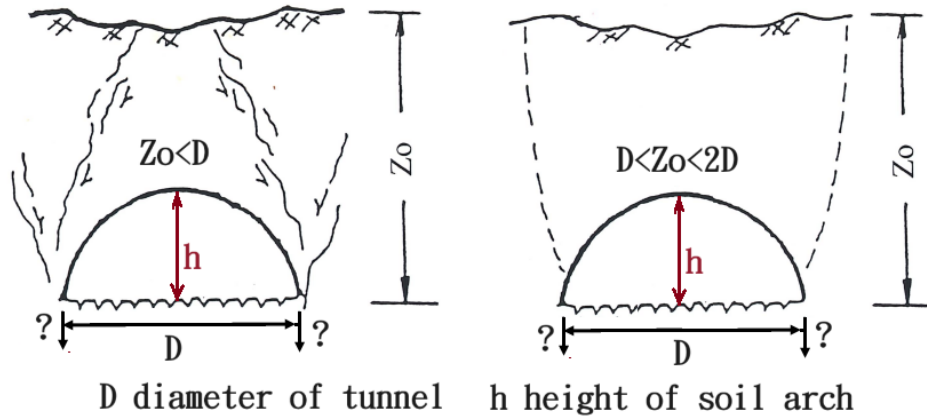


Figure 12. Failure mode of tunnel with shallow overburden (Bair 2002)

6. Conclusions

For the stability analysis of tunnel excavation in weak ground, if the 2D analysis model is used and the groundwater pressure is fixed, under the temporary support of steel wire mesh shotcrete and steel support, the analysis result is in a stable state, but the 2D analysis model cannot present the stable state of the face. Especially, seepage force affects stability of the face. The seepage force can take away the fine particles, resulting in an unstable state during the excavation of the tunnel.

Therefore, for the stability analysis of tunnel excavation in sandy soil and silt soil, 3D models and fluid-mechanical coupling (or seepage) should be used for stability analysis. During the excavation process of the connection way, the decline of groundwater is conducive to the stability of the face of the connection way, which cannot be presented in the stability analysis that generally does not consider fluid-mechanical coupling or seepage.

References

- Wan Lianju et al., *Engineering Seepage Mechanics and Its Application*, China Building Materials Industry Press, 2001.
- Bair Jin Yueih., *Is a full face drive safer and more effective than sequential excavation in mixed ground?* ITA-AITES World Tunnel Congress (WTC) 2020 and 46th General Assembly, Malaysia, 2020.
- Arnold Verruit., *THEORY AND PROBLEMS OF POROELASTICITY*, Delft University of Technology, pp.2-11, 2016.
- Andi Merxhani., *An introduction to linear poroelasticity*, 2016.
- Bair Jin Yueih., *Tunnel Risk Analysis and Advance Rate Assessment*, Engineering, February, PP.78-91, 2002.